

Emergence of coexisting coherence and incoherence by an external forcing

V. K. Chandrasekar¹, R. Suresh¹, D. V. Senthilkumar^{1,*} and M. Lakshmanan²

¹Centre for Nonlinear Science and Engineering, School of Electrical and Electronics Engineering, SASTRA University, Thanjavur 613 401, India

²Centre for Nonlinear Dynamics, School of Physics, Bharathidasan University, Tiruchirappalli 620 024, India

(Dated: November 9, 2021)

A common external forcing can cause a saddle-node bifurcation in an ensemble of identical Duffing oscillators by breaking the symmetry of the individual bistable (double-well) unit. The strength of the forcing determines the separation between the saddle and node, which in turn dictates different dynamical transitions depending on the distribution of the initial states of the oscillators. In particular, chimera-like states appear in the vicinity of the saddle-node bifurcation for which theoretical explanation is provided from the stability of slow-scale dynamics of the original system of equations. Further, as a consequence, it is shown that even a linear nearest neighbor coupling can lead to the manifestation of the chimera states in an ensemble of identical Duffing oscillators in the presence of the common external forcing.

PACS numbers: 05.45.Xt, 89.75.-k, 05.45.-a

Ensembles of coupled oscillators are veritable black boxes which have been widely employed to understand a plethora of collective/co-operative dynamics observed in diverse natural systems [1–3]. Identification of simultaneous existence of a group of oscillators in harmony while the rest in dissonance in an ensemble of coupled identical oscillators has resulted in the notion of “chimera” states [4]. Since the first identification of the coexistence of coherence and incoherence by Kuramoto and Battogtokh [5], many exciting developments have been made, including a number of experimental demonstrations [6–8]. A flurry of recent investigations revealed nonlocal coupling as a basic criterion for the onset of chimera in phase reduced models under weak coupling limit [4, 5], and also in systems far from the weak coupling limit [9]. Very recently, the above limitation on the existing criterion for the onset of chimera has been liberalized to include an ensemble of globally coupled oscillators [10–12]. Nevertheless, the mechanism for the birth of chimera states in an ensemble of identical oscillators has been shown as the emergence of multistability in both nonlocal and global coupling configurations [4, 5, 9–12]. However, it is not clear whether the converse is true, that is whether chimera can occur in a given multistable system either with nonlocal or with global coupling or even with much simpler couplings such as linear nearest neighbor coupling. A general criterion for the onset of chimera states in such dynamical systems is yet to be unraveled.

A periodically driven oscillator is the main and historically first studied model in the classical theory of synchronization, where a triode generator is synchronized by a weak external periodic signal [14]. In reality, there exists a variety of instances where the onset of such a collective behavior is invoked by an external force [1–3]. Examples include, phase locking of electrically decoupled spin torque nano oscillators (STNOs) by an applied external microwave magnetic field [15, 16], polariton condensates in semiconductor microcavities that interact with the reservoir [17], frequency controlled devices, synchronization of micromechanical oscillators using light [18], etc. Here, we first consider an ensemble

of identical bistable systems driven by a common external force without establishing any explicit coupling between the systems and investigate the underlying dynamics of the ensemble (or equivalently, that of an identical system for an ensemble of different initial conditions) as a function of the strength of the forcing. Then we investigate the effect of coupling leading to the manifestation of chimera states.

The collective steady states resulting from the basin of attraction of the ensemble of identical oscillators (or an ensemble of initial conditions) provides a clue about the basic criterion for the onset of chimeras in the ensemble of such systems with coupling. In particular, we find that if the basin of attraction of a bistable (multistable) system leads to coexisting attractors of distinctly different nature under a common forcing, the ensemble of such systems will immediately lead to the onset of chimera near the saddle node bifurcation of the ensemble under coupling. For appropriate forcing amplitude, the basin of attraction of the bistable system has essentially two domains of attraction. Initial conditions from one of the domains (coherent domain) lead to the same (chronotaxic [19]) attractor while that of the other domain (incoherent domain) lead to quasiperiodic/chaotic attractors. Thus the collective steady state dynamics, whose initial conditions are uniformly distributed in the two domains, emerging from the basin of attraction resembles the chimera states under the common external forcing. In the following, we will show as a general criterion that if the basin of attraction of a given dynamical system displays coexisting coherent and incoherent domains of attraction under the common external forcing, then even a linear nearest neighbor coupling can lead to the manifestation of chimera states in the ensemble of identical systems even for a low coupling strength in the same parameter space. This approach will be extremely useful, and provides a cost-effective way in laboratory experiments to confirm the emergence of chimeras with just a single oscillator before experimenting with an ensemble of oscillators. In addition, the ensemble of identical oscillators driven by a common forcing opens up the possibility of analytical treatment which we will carry out

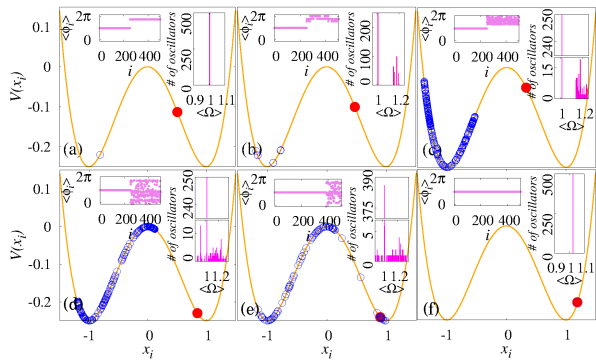


FIG. 1: (Color online) Distribution of the ensemble ($N = 500$) of Duffing oscillators in a double-well potential along with their average phase and average frequency distribution in the insets. (a) $f_e = 0$, (b) $f_e = 0.088$, (c) $f_e = 0.135$, (d) $f_e = 0.15$, (e) $f_e = 0.16$ and (f) $f_e = 0.19$. See text for explanations.

in the following.

In this Rapid Communication, we consider a bistable system with double-well potential as an individual oscillator exhibiting reflection symmetry which undergoes a pitch-fork bifurcation [20] as a function of the system parameter. The basin of attraction of the ensemble of such identical oscillators leads to two cluster states corresponding to the bistable attractors with reflection symmetry. The common external force then leads to a saddle-node bifurcation of the ensemble by breaking the reflection symmetry of the individual oscillators. For suitable values of the amplitude of the external force near the saddle-node bifurcation, we find the co-existence of coherent and incoherent steady states among the oscillator ensemble mimicking chimera states. Using a slow-scale approximation and the method of direct separation [13], we separate the slow-scale dynamics from the original system of equations. The stability of the steady state solutions of the slow-scale dynamics provides an appropriate theoretical explanation for the observed dynamical transitions in the simulation.

In general, an oscillator with a double-well potential of the form $V(x) = x^4 - x^2$ will have two stable fixed points and one unstable fixed point exhibiting bistability. A well known paradigmatic oscillator with this type of potential is the classical model of Duffing oscillator [21], the ensemble of which with a common force is represented by

$$\begin{aligned} \ddot{x}_i + \alpha \dot{x}_i - \omega_0^2 x_i + \beta x_i^3 - f \sin(\omega t) \\ = f_e \sin(\omega_e t), i = 1, 2, \dots, N \end{aligned} \quad (1)$$

where $\alpha = 0.5$, $\omega_0 = 1$, $\beta = 1$, $\omega = 1$ and $f = 0.33$ are the system parameters for which the individual Duffing oscillator, in the absence of the external force ($f_e = 0$), exhibits periodic oscillations with period $T \approx \frac{2\pi}{\omega}$, $\omega_e = 0.5$ is the frequency of the external forcing. We have fixed the number of oscillators as $N = 500$ and the system parameters as above throughout the manuscript. The Duffing oscillator has been investigated in great detail for its dynamical behavior with and without an

additional external forcing for its chaotic nature and resonance phenomenon [21].

Initial conditions of the ensemble of identical oscillators are uniformly distributed in both the wells with equal probability in our simulation. Without any additional external force ($f_e = 0$) the ensemble of individual oscillators will be oscillating synchronously in either of the wells as depicted in Fig. 1(a). However, the oscillators in both the wells exhibit out-of-phase oscillations with each other while oscillating with the same frequency $\omega = 1$ (see insets of Fig. 1(a)) due to the symmetry property of Eq. (1). With the addition of the common external force to the ensemble, the synchronized oscillators in one of the wells desynchronize to form self organized clusters with distinct frequencies (see insets of Fig. 1(b)), while the oscillators in the other well remain synchronized as shown in Fig. 1(b) for $f_e = 0.088$. Increasing the amplitude of the external force to $f_e = 0.135$, the self organized clusters desynchronize completely (Fig. 1(c)). Thus the splitting of the basin of attraction of an ensemble of identical oscillators, for appropriate values of external forcing amplitude, into coherent and incoherent domains under the influence of a common external forcing leads to the existence of chimera-like states.

Upon increasing f_e further, we find that the desynchronized oscillators hop back and forth to the other well where the synchronized group resides, the snap shot of which is depicted in Fig. 1(d) for $f_e = 0.15$ again representing the chimera-like state. It is evident from Figs. 1(c) and 1(d) that the desynchronized group remains confined to one of the wells for $f_e = 0.135$ and gets distributed in both the wells for $f_e = 0.15$, thereby distinguishing two distinct chimera-like states C-I and C-II, respectively. The phase and frequency of the desynchronized group are clearly distinct from that of the synchronized group in the former case (see insets of Fig. 1(c)), whereas they are distributed about the phase and frequency of the synchronized group in the latter case as depicted in the insets of Figs. 1(d) and (e). Some of the mobilized desynchronous oscillators are trapped in the other well to form a large cluster of synchronized oscillators for further larger values of the amplitude of the external forcing. For $f_e = 0.16$, increase in the size of synchronized group is corroborated from the degree of phase and frequency distribution as in Fig. 1(e). Finally, the desynchronized oscillators are all attracted to the other well to form a single synchronized cluster for $f_e = 0.19$ as illustrated in Fig. 1(f). Thus the ensemble of bistable oscillators loses its bistability to become monostable by switching the stability of one of the stable fixed points via the chimera-like states as a function of f_e . Existence of analogous chimera states between two populations with both inter- and intra-global couplings, as employed by Abrams et al [22], has been demonstrated in discrete chemical oscillators based on the photosensitive Belousov-Zhabotinsky (BZ) reaction by Tinsley et al [6] and in mechanical oscillator networks by Martens et al [7]. Interestingly, we have observed similar transitions even in the states emerging from the basin of attraction of an ensemble of identical bistable oscillators driven

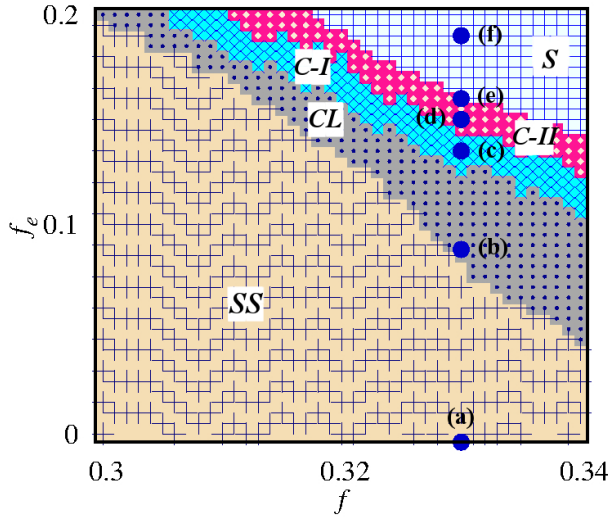


FIG. 2: (Color online) Two parameter ($f - f_e$) phase diagram demarcating various dynamical regimes. See text for details.

by a common force.

To obtain a global perspective, we have depicted the $f - f_e$ two parameter phase diagram in Fig. 2. The parameter space corresponding to the collective steady state dynamical behaviors discussed in Figs. 1(a)-(f) are labeled as (a)-(f) in Fig. 2. The steady states exhibit synchronous oscillations in either of the wells depending on the distribution of the initial conditions in the region marked as ‘SS’. Clusters of synchronous oscillators are seen in one of the wells in the region indicated by ‘CL’. Two distinct chimera-like states are observed in the regions denoted by ‘C - I’ and ‘C - II’, respectively. Synchronized single-well oscillations are found in the parameter space ‘S’.

To explore the reason behind the observed transitions, we start with the dynamics of Eq. (1) without any forcing. For $f = f_e = 0$, Eq. (1) has two stable fixed points and one unstable fixed point. Depending upon the distribution of the initial states, the ensemble of oscillators is attracted towards either of the stable fixed points. For finite values of f , the oscillators corresponding to the stable fixed points oscillate in opposite phase but with the same frequency, observed in Figs. 1(a) and 2(a), in the asymptotic ($t \rightarrow \infty$) limit because of the invariant condition $(x_i, f \sin(\omega t)) \rightarrow (-x_i, f \sin(\omega t + \pi))$. Now, using the multi-time scale perturbation theory [13] and introducing a small parameter $\varepsilon \ll 1$ as $(\alpha, \omega_0, \beta, f_e) \rightarrow \varepsilon(\alpha, \omega_0, \varepsilon\beta, \varepsilon f_e)$, the solution for Eq. (1) can be separated as $x_i(t) = y_i(\omega t) + z_i(\varepsilon t)$, where $y_i(\omega t) = -\frac{f}{\omega^2} \sin(\omega t)$ is the solution of Eq. (1) for $f_e = 0$ by neglecting the higher harmonics, and $z(\varepsilon t)$ is a slow time scale perturbation. Plugging $x_i(t) = y_i(\omega t) + z_i(\varepsilon t)$ in Eq. (1) and averaging over 0 to $\frac{2\pi}{\omega}$, we obtain

$$\ddot{z}_i + \alpha \dot{z}_i + (F^2 - \omega_0^2)z_i + \beta z_i^3 = F_e, \quad (2)$$

where $\langle x \rangle = \frac{\omega}{2\pi} \int_0^{\frac{2\pi}{\omega}} x dt = z$, $F^2 = \frac{3\beta f^2}{2\omega^4}$ and $F_e =$

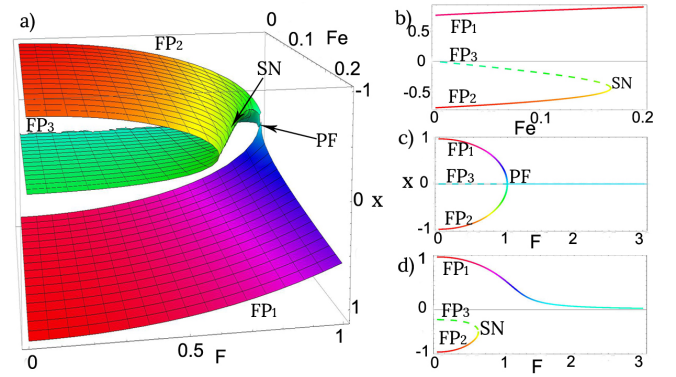


FIG. 3: (Color online) Analytical stability diagrams. (a) Profile of the fixed points of the slow-scale dynamical equation, Eq. (2), (b) Level curve of Fig. 3(a) depicting saddle-node bifurcation of the ensemble of oscillators for $F = 0.65$, (c) Level curve of Fig. 3(a) for $F_e = 0.0$ showing pitch-fork bifurcation of the individual oscillators, and (d) Level curve of Fig. 3(a) for $F_e = 0.2$ illustrating saddle-node bifurcation of the ensemble of oscillators. FP1, FP2 and FP3 refer to the three fixed point solutions of Eq. (2).

$\langle f_e \sin(\omega_e t) \rangle$ is non-zero for non-integer values of $\frac{\omega_e}{\omega}$ breaking the reflection (left-right) symmetry leading to saddle-node bifurcation around which the dynamical transitions occur. Equation (2) has three fixed points (a saddle and two stable foci/nodes) for $F_e < F_{c,\pm} = \pm \frac{2(\omega_0^2 - F^2)^{\frac{3}{2}}}{3\sqrt{3}\beta}$. The stability and the nature of the above fixed points determines the observed dynamical transitions discussed in Figs. 1 and 2. Profiles of the fixed points of Eq. (2) is depicted in Fig. 3(a) as a function of F and F_e . The stable fixed points are symmetric about the saddle for $F_e = 0$ (see Fig. 3(a)), whereas upon increasing F_e one of the stable (negative) fixed points and the saddle converge towards each other to merge at $F_e = F_{c,+}$ via saddle-node bifurcation as depicted in Fig. 3(a). Conversely, the stable (positive) fixed point and the saddle can also converge towards each other to merge at $F_e = F_{c,-}$. This means if F is replaced by $-F$, then we observe similar dynamics but in the other well. The fixed point profile for $F = 0.65$ is shown in Fig. 3(b) as a function of F_e . It is evident from both Figs. 3(a) and (b) that the separation between the saddle and the stable (negative) fixed point decreases monotonically upon increasing F_e , while the other fixed point remains unaltered. The degree of separation and the distribution of the initial states of the ensemble of oscillators altogether determine the nature of dynamical transitions as a function of the forcing.

Cluster states are formed in a range of F_e for fixed F depending on the degree of repulsion exerted by the saddle on the ensemble of oscillators whose initial states are distributed in the vicinity of the saddle and the stable fixed point. Such cluster states are represented in Fig. 1(b). Indeed cluster states are formed in both the wells even for $F_e = 0$ ($f_e = 0$) but for large values of F (f) as can be seen in Fig. 2. However, states mimicking chimera do not exist for $F_e = 0$ because both the fixed points approach the saddle resulting in complete inco-

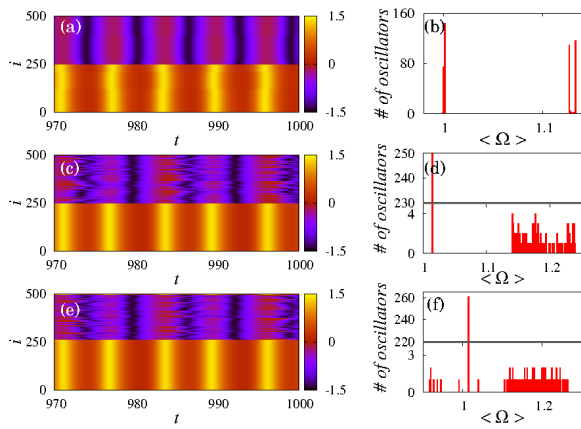


FIG. 4: (Color online) Spatiotemporal plots (left column) and probability distribution of time averaged frequency (right column) of an ensemble of Duffing oscillators with linear nearest neighbor coupling in the presence of the common external forcing depicting (a)-(b) cluster states for $\varepsilon = 0.06$ and $f_e = 0$, (c)-(d) chimera-like states for $\varepsilon = 0.0$ and $f_e = 0.14$, and (e)-(f) chimera states for $\varepsilon = 0.06$ and $f_e = 0.14$.

herent oscillations in both the wells for large F [21]. Finally, the fixed points collide with the saddle to create a new stable fixed point through pitch-fork bifurcation (see Fig. 3(c)) resulting in double-well oscillations. In contrast, for a finite value of F_e , above $F_e = 0$, the ensemble of oscillators undergo double-well oscillations via cluster, chimera-like states and single-well oscillations, where the symmetry between the fixed points are broken and saddle-node bifurcation occurs at the onset of single-well oscillations as a function of F as depicted in Fig. 3(d) for $F_e = 0.2$.

As the separation between the saddle and the stable fixed point narrows down further on increasing F_e beyond that of the cluster states, the saddle expels the oscillators away from the stable fixed point resulting in incoherence among the oscillators in the well, while the oscillators in the other well are in coherence by which C -I emerges in Fig. 1(c). For further large values of F_e the separation between the saddle and the stable fixed point becomes negligibly small and they eventually merge together to form a saddle-node bifurcation. In this narrow range of F_e (as seen in the two parameter phase diagram in Fig. 2), some of the oscillators whose initial conditions lie in the vicinity of the saddle makes round trip among both the wells and some of them are attracted in their opposite well depending on the value of F_e elucidating the existence of C -II states, which we have observed in Figs 1(d)-(e). Beyond the saddle-node bifurcation, the saddle and stable fixed point disappear only with the existence of the stable positive fixed point in the other well to which all of the oscillators are attracted finally for sufficiently large F_e confirming our discussion on Fig. 1(f).

Now, we will show that even a linear nearest neighbor coupling can lead to the manifestation of chimera states in an ensemble of Duffing oscillators in the presence of the common

external forcing represented as

$$\begin{aligned} \ddot{x}_i + \alpha \dot{x}_i - \omega_0^2 x_i + \beta x_i^3 - f \sin(\omega t) \\ + \varepsilon G = f_e \sin(\omega_e t), i = 1, 2, \dots, N \end{aligned} \quad (3)$$

where ε is the coupling strength and G is the coupling function characterizing the linear nearest neighbor coupling ($x_{i+1} + x_{i-1} - 2x_i$) while the system parameters are the same as in Eq. (1). Spatiotemporal plots and the probability distribution of the time averaged frequency $\langle \Omega \rangle$ are depicted in the left and the right columns of Fig. 4 for various values of the system parameters. In the absence of the common external force $f_e = 0$ the ensemble of Duffing oscillators with nearest neighbor coupling displays cluster states as shown in Figs. 4(a) and (b) for the coupling strength $\varepsilon = 0.06$. The ensemble will exhibit chimera-like states, as discussed above, when driven by the common external forcing in the absence of any couplings ($\varepsilon = 0.0$) between the oscillators (see Figs. 4(c) and (d)) for $f_e = 0.14$. Chimera states manifest even due to a linear nearest neighbor coupling in the presence of the common external forcing as shown in Figs. 4(e) and (h). The spatiotemporal plot and the probability distribution of $\langle \Omega \rangle$ is depicted in Figs. 4(e) and (f), respectively, for the coupling strength $\varepsilon = 0.06$ and the forcing amplitude $f_e = 0.14$. It is clear from these figures that there is a simultaneous emergence of synchronized and desynchronized domains among the ensemble of identical Duffing oscillators elucidating the existence of chimera states due to the nearest neighbor coupling in the presence of the common external force in the same parameter regime where chimera-like states are observed without coupling. The effect of nearest neighbor coupling is clearly evident from Fig. 4(f), where there is a shift in the frequency of the synchronized domain compared to that of the chimera-like states in Fig. 4(d), while the frequency of the desynchronized domain has a much wider distribution than that of the chimera-like states. Thus it is evident that the chimera state manifests due to the nearest neighbor coupling but in the presence of the common external force. Chimera states emerge even for such a low value of coupling strength $\varepsilon = 0.06$, essentially because of the precursor chimera-like states in the absence of coupling. The above results indicate that even an ensemble of oscillators with linear nearest neighbor coupling can exhibit chimeras under suitable conditions. Note that the system (3) can also be interpreted as an ensemble of Duffing oscillators with double forcing and with linear nearest neighbor coupling. We have further verified the generic nature of our results in ensembles of Stuart-Landau oscillators and Rössler oscillators in the presence of the common external forcing, the details of which will be published elsewhere.

To summarize, surprisingly we have found that the basin of attraction of an ensemble of identical bistable oscillators can indeed display coexisting coherent and incoherent domains with distinctly different nature of attractors mimicking chimera states under a common forcing, even without any explicit coupling, using Duffing oscillator as a typical example.

The common force facilitates a global saddle-node bifurcation of the ensemble by breaking the symmetry of the individual oscillators exhibiting pitch-fork bifurcation in the absence of the external forcing. The spontaneous splitting of the ensemble is found to emerge near the saddle-node bifurcation under an appropriate forcing. We have also provided an appropriate analytical treatment of the original system of equations, where we have separated the slow-scale dynamics and investigated the stability of the underlying fixed points, which provides necessary explanation confirming the observed dynamical transitions in the simulation. Further, it is also shown that even a linear nearest neighbor coupling can lead to the manifestation of the chimera states in an ensemble of identical Duffing oscillators but in the presence of the common external forcing. As driving/influencing others is a natural behavioral tendency in ecology such as in a herd of sheep, flock of birds, colony of ants, hive of bees and many more, as well as in epidemics, in neuroscience, in social networks, etc., there lies every possibility that such an emergent behavior may exist in several natural systems. Our results may open up potential activities in the identification of chimera states in appropriate natural systems. In particular, our results have elucidated that still there are new avenues open to extend the horizon of the existence criteria for the framework of chimera with more simple and realistic couplings/situations that fits with the real world examples. More significantly, our results will serve as a basic framework to ensure the existence of chimeras in laboratory systems before performing experiments using ensembles of such systems.

The work of VKC is supported by INSA young scientist project. DVS is supported by the SERB-DST Fast Track scheme for young scientist under Grant No. ST/FTP/PS-119/2013. ML is supported by a Department of Science and Technology (DST), Government of India, IRHPA research project. ML is also supported by a DAE Raja Ramanna Fellowship.

* Electronic address: skumarusnld@gmail.com

- [1] A. Pikovsky, M. Rosenblum, and J. Kurths, *Synchronization: A Universal Concept in Nonlinear Sciences* (Cambridge University Press, Cambridge, 2001); and references therein.
- [2] A. T. Winfree, *The Geometry of Biological Time* (Springer-Verlag, Berlin, Germany, 1980).
- [3] M. Lakshmanan and D. V. Senthilkumar, *Dynamics of Nonlinear Time-Delay Systems* (Springer, Berlin, 2010).
- [4] Y. Kuramoto and D. Battogtokh, *Nonlinear Phenom. Complex Syst.* **5**, 380 (2002); S. I. Shima and Y. Kuramoto, *Phys. Rev. E* **69**, 036213 (2004); D. M. Abrams and S. H. Strogatz, *Phys. Rev. Lett.* **93**, 174102 (2004); D. M. Abrams and S. H. Strogatz, *Int. J. Bif. Chaos* **16**, 21 (2006); E. A. Martens, C. R. Laing, and S. H. Strogatz, *Phys. Rev. Lett.* **104**, 044101 (2010).
- [5] Y. Kuramoto and H. Nakao, *Phys. Rev. Lett.* **76**, 4352 (1996); *Physica D* **103**, 294 (1997); Y. Kuramoto, D. Battogtokh, and H. Nakao, *Phys. Rev. Lett.* **81**, 3543 (1998).
- [6] M. R. Tinsley, S. Nkomo, and S. Showalter, *Nat. Phys.* **8**, 662 (2012).
- [7] E. A. Martens, S. Thutupalli, A. Fourriere, and O. Hallatschek, *Proc. Nat. Acad. Sciences* **110**, 10563 (2013).
- [8] L. Larger, B. Penkovsky, and Y. L. Maistrenko, *Phys. Rev. Lett.* **111**, 054103 (2013); M. Wickramasinghe and I. Z. Kiss, *PLoS ONE* **8**, e80586 (2013); T. Kapitaniak, P. Kuzma, J. Wojewoda, K. Czołczynski, and Y. L. Maistrenko, *Scientific Reports* **4**, 6379 (2014); E. A. Viktorov, T. Habruseva, S. P. Hegarty, G. Huyet, and B. Kelleher, *Phys. Rev. Lett.* **112**, 224101 (2014); L. Schmidt, K. Schofleber, K. Krischer, and V. Garcia-Morales, *Chaos* **24**, 013102 (2014); L. Larger, B. Penkovsky, and Y. L. Maistrenko, arXiv 1411.4483, (2014); Fabian Böhm, Anna Zakharova, Eckehard Schöll, and Kathy Lüdge, arXiv:1412.0957, (2014).
- [9] I. Omelchenko, Y. Maistrenko, P. Hövel, and E. Schöll, *Phys. Rev. Lett.* **106**, 234102 (2011); I. Omelchenko, B. Riemenschneider, P. Hövel, Y. Maistrenko, and E. Schöll, *Phys. Rev. E* **85**, 026212 (2012); I. Omelchenko, O. E. Omelchenko, P. Hövel, and E. Schöll, *Phys. Rev. Lett.* **110**, 224101 (2013); G. C. Sethia, A. Sen, and G. L. Johnston, *Phys. Rev. E* **88**, 042917 (2013); S. R. Ujjwal, and R. Ramaswamy, *Phys. Rev. E* **88**, 032902 (2013); D. Pazo, and E. Montbrío, *Phys. Rev. X*, **4**, 011009, (2014); R. Gopal, V. K. Chandrasekar, A. Venkatesan, and M. Lakshmanan, *Phys. Rev. E* **89**, 052914 (2014); Anna Zakharova, Marie Kapeller, Eckehard Schöll, *Phys. Rev. Lett.* **112**, 154101 (2014); D. Dudkowski, Y. Maistrenko, and T. Kapitaniak, *Phys. Rev. E* **90**, 032920 (2014).
- [10] G. C. Sethia and A. Sen *Phys. Rev. Lett.* **112**, 144101 (2014).
- [11] A. Yeldesbay, A. Pikovsky, and M. Rosenblum, *Phys. Rev. Lett.* **112**, 144103 (2014).
- [12] V. K. Chandrasekar, R. Gopal, A. Venkatesan, and M. Lakshmanan, *Phys. Rev. E* **90**, 062913 (2014).
- [13] A. Fidlin, *Nonlinear Oscillations in Mechanical Engineering* (Springer-verlag, Berlin, 2006); I. I. Blekhman, *Vibrational Mechanics: Nonlinear Dynamic Effects, General Approach, Applications* (World Scientific, Singapore, 2000).
- [14] E. V. Appleton, *Proc. Cambridge Phil. Soc. (Math and Phys. Sci.)* **21**, 231 (1922); B. Van der Pol, *Phil. Mag.* **3**, 64 (1927).
- [15] S. Kaka, M. R. Pufall, W. H. Rippard, T. J. Silva, S. E. Russek, and J. A. Katine, *Nature* **437**, 389 (2005).
- [16] B. Subash, V. K. Chandrasekar, and M. Lakshmanan, *Eur. Phys. Lett.* **102** 17010, (2013).
- [17] M. Wouters, *Phys. Rev. B* **77**, 121302(R) (2008).
- [18] Dario Antonio, Damin H. Zanette, and Daniel Lopez, *Nat. Commun.* **3**, 806 (2012); M. Zhang, G. S. Wiederhecker, S. Manipatruni, A. Barnard, Paul McEuen, and M. Lipson, *Phys. Rev. Lett.* **109**, 233906 (2012).
- [19] Y. F. Suprunenko, P. T. Clemson and A. Stefanovska, *Phys. Rev. Lett.* **111**, 024101 (2013)
- [20] S.-Y. Kim, and Y. Kim, *Phys. Rev. E* **61**, 6517 (2000); Y. Kim, S.-Y. Lee, S.-Y. Kim, *Phys. Lett. A* **275**, 254 (2000).
- [21] A. H. Nayfeh and D. T. Mook, *Nonlinear-Oscillations* (John Wiley & Sons, New York 1995); M. Lakshmanan and S. Rajasekar, *Nonlinear Dynamics: Integrability, Chaos and Patterns*, (Springer-Verlag, New York, 2003); I. Kovacic, and M. J. Brennan, *The Duffing Equation- Nonlinear Oscillators and Their Behaviour* (John Wiley & Sons, New York 2011).
- [22] D. M. Abrams, R. Mirollo, S. H. Strogatz, and D. A. Wiley, *Phys. Rev. Lett.* **101**, 084103 (2008).
- [23] I. I. Blekhman, and P. S. Landa, *Int. J. Nonlinear Mechanics* **39**, 421 (2004); P. S. Landa, and P. V. E. McClintock, *J. Phys. A* **33**, L433 (2000).